

Associative ionization in collisions of He^+ with H^- and D^-

A Naji[†], K Olamba[†], J P Chenu[†], S Szücs[†], M Chibisov[‡] and F Brouillard[†]

[†] Université Catholique de Louvain, Département de Physique, Unité de Physique Atomique et Moléculaire, Chemin du cyclotron, 2, B-1348 Louvain-la-Neuve, Belgium

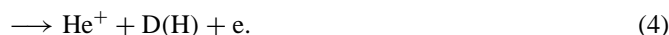
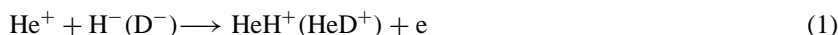
[‡] Russian Research Center, Kurchatov Institute, Institute of Nuclear Fusion, 123182 Moscow, Kurchatov str. 1, Russia

Received 18 March 1998, in final form 8 May 1998

Abstract. Absolute cross sections of the associative ionization in the collision of He^+ with H^- or D^- have been measured in a merged beam experiment over a relative velocity interval ranging from 0.4 to $5 \times 10^6 \text{ cm s}^{-1}$. At a given relative velocity, the two cross sections significantly differ at low velocities where the cross section for HeD^+ formation exceeds that of HeH^+ by as much as 35%. The difference, however, decreases with the velocity and falls in the experimental error above $2 \times 10^6 \text{ cm s}^{-1}$. In both cases the energy dependence becomes compatible at low energy with an E^{-1} law.

1. Introduction

In collisions of He^+ with H^- and D^- , several processes can take place. At low collision energy, associative ionization is one of them, the others being mutual neutralisation, transfer ionization and direct detachment



A complete understanding of the dynamics of collisions of He^+ with H^- or D^- requires both experimental and theoretical studies of reactions (1)–(4) and of their reverse processes because they compete and possibly interfere. For example, the cross section of mutual neutralization can decrease at low energy as a result of associative and transfer ionization and at high collision energy as a result of direct detachment.

Mutual neutralization (reaction (2)) has been investigated both experimentally and theoretically by Gaily *et al* [1], Peart *et al* [2, 3], Ermolaev *et al* [4], Olamba *et al* [5] and Chibisov *et al* [6].

The collision of metastable He with H and D leading to the same products as (1) and (4) has also been investigated both experimentally and theoretically by Howard *et al* [7], Neynaber *et al* [9, 12], Hickman *et al* [10], Magnuson *et al* [8], Fort *et al* [11] and Waibel *et al* [13].

Some reverse processes such as dissociative recombination of HeH^+ have also been reported by Orel *et al* [14, 15] and Strömholm *et al* [16].

This paper deals with an experimental study of the associative ionization of He^+ with H^- or D^- for collision energies ranging from 0.02 up to about 10 eV. The reported measurements

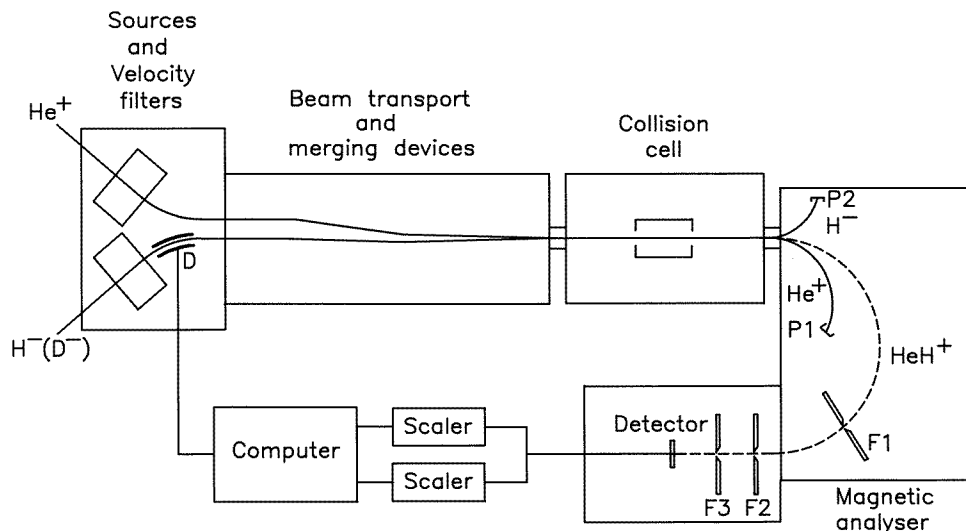


Figure 1. A schematic block diagram of the experimental set-up.

are, as far as we know, the first ones for the absolute cross section of these reactions. Their relation to similar measurements or theoretical studies is briefly commented on.

2. Experimental set-up

The experimental set-up used in these measurements has been described previously [5] and only the main lines are resumed here. The apparatus is shown schematically in figure 1. Four sections are distinguished. The first section includes the ion sources, the acceleration voltages, the beam forming optics and the mass selection. The second is the one where the beams are merged. The third section is the interaction region. The last one contains the magnetic analyser where the intensities of the primary beams are monitored and the reaction products detected.

In summary, the He^+ beam is produced by an electron cyclotron resonance (ECR) source and the negative beam H^- or D^- by a duoplasmatron. The beams are then mass analysed and pure He^+ and H^- or D^- beams are selected. The beams are subsequently diaphragmed and their dimensions defined. They are electrostatically deflected and merged before reaching the interaction region where they interact. At this point, all He^+ ions are essentially in their ground state because metastable ions have been quenched by the electric fields in the acceleration region and in the mass selector, and other excited states have had enough time ($>1 \mu\text{s}$) to decay [5]. The interaction region consists of an electrically biased cell called the observation cell and some probes and beam measuring devices. Finally, a variable (0–4000 G) magnetic field allows one to separate the reaction product (molecular ion) from the primary beams. The molecular ions HeH^+ or HeD^+ are counted by a channel electron multiplier. All these ions are reaching the detector because there is no scattering in associative ionization so that the angular dispersion of the products is similar to that of the parent beams, i.e. less than 2 mrad, thus much smaller than the angular acceptance of the detector ($>10 \text{ mrad}$).

3. Experimental procedure

When using merged beams for absolute cross section measurements, the number of reactions occurring during a time T is given [5] by the expression

$$N(T) = \sigma \frac{v}{q_1 q_2 v_1 v_2} \int_0^T dt \int_V I_1(t) I_2(t) F(t) dt \quad (5)$$

where v_1 , v_2 , q_1 , q_2 , I_1 , I_2 , v are the velocities of the two beams, their charges, their intensities and their relative velocity. σ is the cross section of the reaction and

$$F(t) = \int_0^L F(z, t) dz \quad (6)$$

is the so-called form factor, the factor $F(z, t)$ being defined as

$$F(z, t) = \frac{\int \int j_1(x, y, z, t) j_2(x, y, z, t) dx dy}{I_1(t) I_2(t)} \quad (7)$$

where j_1 and j_2 are the current densities. In order to derive the cross section σ , from the measured number of reactions $N(T)$, one has to know the form factor $F(t)$, that accounts for the degree of overlap of the beams.

The knowledge of the form factor involves the measurement of the density profiles of the two beams. Presently this is conveniently done thanks to the computer-assisted measurement of the beam profiles described in [5]. The form factor, however, reduces to a very simple expression if the beams have a sharply defined section, with uniform density and are fully merged over a known length. Then,

$$F = \frac{L}{S_{>}} \quad (8)$$

here $S_{>}$ denotes the section of the largest beam and L the length over which the beams usefully interact (by usefully we mean that the reaction products can reach their detector). These conditions are easily fulfilled by strongly diaphragming the beams just before they interact, thus only using the core of the incoming beams. This is of course at the expense of the intensity and is only feasible if the available intensities are large and can be strongly reduced without prohibitively affecting the reaction rate. This was the case in these measurements which were therefore carried out in this way, giving the two beams the same final section by means of a common diaphragm inserted in the merged section, in front of the observation cell. The results were checked now and then by comparing them with those obtained using the form factor. No significant difference was ever found.

It is important to mention here how the interaction length L is defined. The interaction length L is defined by applying a voltage V on the observation cell. As a result molecular ions formed in the cell have their kinetic energy raised by an amount eV and are separated in the magnetic analyser from molecular ions formed elsewhere. The length L is therefore equal to that of the region where the electric potential is equal to V within a margin determined by the energy resolution of the analyser. Thus, knowing the latter, the interaction length is defined with an accuracy limited by the energy dispersion of the beams (of the order of 10 eV).

The observation voltage also determines the barycentric energy E_{cm} :

$$E_{\text{cm}} = \mu \left[\sqrt{\frac{q_2(A_2 - V)}{m_2}} - \sqrt{\frac{q_1(A_1 - V)}{m_1}} \right]^2 \quad (9)$$

A_1 and A_2 are the acceleration voltages of the H^- (D^-) and He^+ beams. m_1 and m_2 are the masses of H^- and He^+ respectively and μ is the reduced mass.

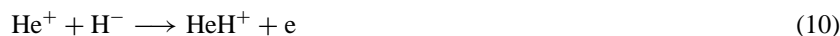
Thus a fine adjustment of the collision energy can be achieved by changing the observation voltage.

The number of reactions $N(T)$ is obtained by measuring the number of counts on the detector. In contrast to our previous measurements no coincident detection is used in this case, so that backgrounds must be strongly suppressed. Fortunately, the molecular ion can only be produced by the mutual interaction of the beams and not by their interaction with the residual gas. However, an important background is created by the elastic scattering of the primary ions especially in the magnetic analyser and also by photon emission at the impact on surfaces. This background was reduced to an acceptable level (typically three times the signal) by the use of shielding elements as the slits $F2$ and $F3$ shown in figure 1.

The background contribution was measured by chopping the negative ion beam by means of a crenel voltage applied on the deflector D and recording the count rate with the negative beam both on and off. It has been checked that the negative beam by itself does not create any background and that the background is identical whether the negative beam is on or off. In these circumstances, the number of molecular ions is obtained as the difference between the number of counts recorded during the same time with the negative ion beam on and off.

4. Results and comments

The associative ionization cross sections of the reactions



have been measured at collision energies ranging from 0.02 to 10 eV. Typical experimental conditions are given in table 1.

A summary of the main factors limiting the accuracy of the present measurements is given in table 2 together with the corresponding errors. The detection efficiency η has been measured using H^+ ions and was found to be 95% at 5 keV [18], that is at a velocity similar to that of the molecular ions detected in these measurements. The efficiency for the latter ions can only be larger and is thus in the range 95–100%. The cross sections have been calculated using $\eta = 98\%$ allowing for a possible error of $\pm 2\%$. The statistical error associated with the observed number of reactions comes in addition. For most of the points, it was about 10% (90% confidence level).

Table 1. Typical experimental conditions.

Beam acceleration voltages	from 6 to 15 kV
Observation voltage	$\simeq -2$ kV
Beam diameters (common)	0.15 cm
He^+ beam intensity	$\simeq 300$ nA
H^- or D^- beam intensity	$\simeq 100$ nA
Background	$\simeq 2$ Hz
Signal $N(T)$ from 0.02 to 10 eV	from 7 to 0.3 Hz
Interaction length L	6.8 cm
Beam divergence	less than 2 mrad

Table 2. Estimation of the experimental errors.

On detection efficiency η	2%
On interaction length L	3%
On beam intensities	2%

Table 3. Experimental associative ionization cross section in $\text{He}^+ + \text{H}^-$ collisions.

v_r (10^6 cm s^{-1})	E_{cm} (eV)	σ (10^{-16} cm^2)	$\pm \Delta\sigma$
0.489	0.10	0.66	0.08
0.556	0.13	0.50	0.06
0.639	0.17	0.38	0.05
0.693	0.20	0.32	0.04
0.775	0.25	0.29	0.03
0.856	0.31	0.23	0.03
0.979	0.40	0.21	0.02
1.100	0.51	0.16	0.02
1.195	0.60	0.13	0.01
1.384	0.807	0.11	0.01
1.547	1.005	0.09	0.01
1.897	1.513	0.073	0.009
2.180	1.998	0.057	0.008
2.677	3.012	0.039	0.005
3.092	4.018	0.022	0.003
3.452	5.010	0.013	0.002
3.785	6.023	0.006	0.001
4.078	6.990	0.0023	0.0007
4.370	8.027	0.0010	0.0007

In tables 3 and 4 we present the results of the measurement of the absolute cross sections for reactions (10) and (11). In figure 2 we show the two cross sections as a function of the barycentric energy E_{cm} . It appears that the energy dependence is in both cases compatible, at low energy, with an E_{cm}^{-1} law. The deviation from this law, observed at very low energy, can be explained by the limited energy resolution of our measurements.

The energy resolution is limited by the energy spread in each of the interacting beams and by their residual divergence.

The energy spread (ΔE) in the beams is approximately 10 eV. The energies of the beams, at zero barycentric energy, are 4 and 16 keV for H^- and He^+ , respectively. The corresponding spreads of the velocities are thus

$$\Delta v_1 = 1.25 \times 10^{-3} v \quad (12)$$

$$\Delta v_2 = 3 \times 10^{-4} v \quad (13)$$

where v is the common velocity of the reactants. As a result, the relative velocity is not zero but in the range $[0-1.55 \times 10^{-3} v]$. The average value of its square calculated with the assumption that the velocities are uniformly distributed over the spread is found to be equal to $0.7 \times 10^{-6} v^2$. The corresponding barycentric energy is then 0.0005 eV.

On the other hand, the divergence of the beam implies that the velocities of the reactants have a transverse component distributed over the range $0-\alpha v$, where α is the maximum angle between the ion trajectory and the beam axis. As a result, the relative velocity is distributed over the range $0-2\alpha v$. Assuming again a uniform distribution, one finds for the square of

Table 4. Experimental associative ionization cross section in $\text{He}^+ + \text{D}^-$ collisions.

v_r (10^6 cm s^{-1})	E_{cm} (eV)	σ (10^{-16} cm^2)	$\pm \Delta\sigma$
0.121	0.013	8.4	0.9
0.149	0.016	6.9	0.8
0.197	0.028	4.9	0.5
0.244	0.042	3.5	0.4
0.291	0.059	2.6	0.3
0.378	0.099	1.8	0.2
0.443	0.137	1.4	0.2
0.537	0.202	0.8	0.1
0.594	0.247	0.73	0.09
0.655	0.296	0.65	0.08
0.726	0.369	0.55	0.07
0.755	0.398	0.50	0.06
0.849	0.504	0.43	0.06
0.925	0.598	0.34	0.04
1.000	0.699	0.26	0.03
1.066	0.795	0.25	0.03
1.208	1.019	0.21	0.03
1.443	1.456	0.14	0.02
1.680	1.967	0.11	0.01
1.923	2.586	0.09	0.01
2.166	3.284	0.077	0.009
2.402	4.033	0.053	0.006
2.879	5.799	0.037	0.004
3.122	6.819	0.026	0.004
3.384	8.011	0.015	0.002
3.589	9.013	0.011	0.001
3.786	10.024	0.009	0.002

the relative velocity an average value of $\alpha^2 v^2$. The corresponding barycentric energy is now

$$\frac{\mu}{2} \alpha^2 v^2 \quad (14)$$

which, as $\alpha = 2$ mrad in our measurements, amounts to the value 0.013 eV. This value, which is much larger than that associated with the energy spread in the beams, can be regarded as the uncertainty affecting the barycentric energy.

The values of the cross section at very low energies are thus average values that are not expected to reflect the true energy dependence but will tend to a ceiling value, that of the average value over the range 0–0.013 eV.

In figure 3 we present the same cross sections as a function of the relative velocity. The ratio of the cross sections with D^- and H^- is of the order of 1.3 at low velocity and decreases at higher velocity where the difference falls within experimental error. Such an isotopic effect is expected as the number of vibrational states is larger for HeD^+ than for HeH^+ .

There is no theoretical prediction with which our results could be directly compared but there are data, both experimental and theoretical, on a related process: associative ionization in the collision of the neutral species H or D and He ($n = 2$) [7–11, 13]. In figure 4 we show, together with our results, the cross sections for associative ionization of H or D with $\text{He}(2^3\text{S})$



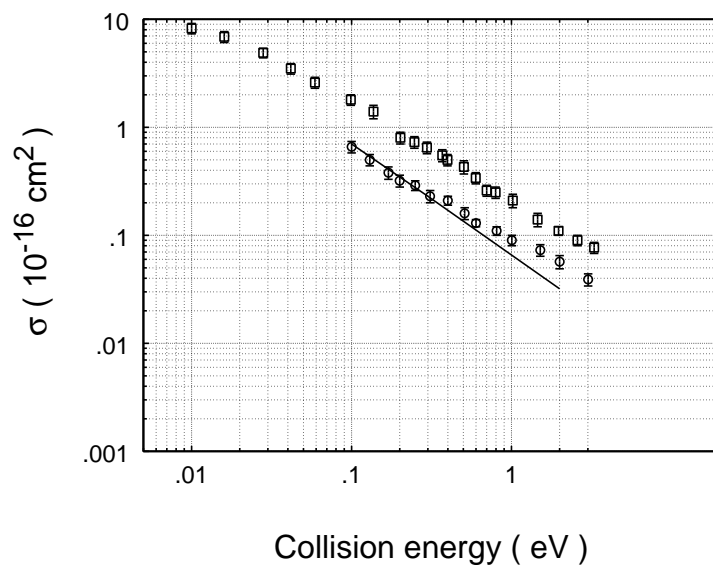


Figure 2. The measured cross sections as a function of the barycentric energy. Open circles: $\text{He}^+ + \text{H}^- \rightarrow \text{HeH}^+ + \text{e}$. Open squares: $\text{He}^+ + \text{D}^- \rightarrow \text{HeD}^+ + \text{e}$. Full line: E_{cm}^{-1} law.

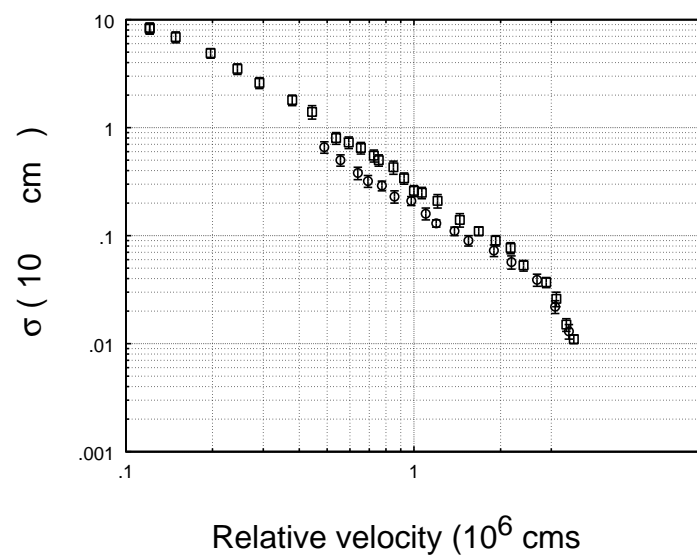


Figure 3. The measured cross sections as a function of relative velocity. Open circles: $\text{He}^+ + \text{H}^- \rightarrow \text{HeH}^+ + \text{e}$. Open squares: $\text{He}^+ + \text{D}^- \rightarrow \text{HeD}^+ + \text{e}$.

as measured by Neynaber and Magnuson [9], Fort *et al* [11] and calculated by Waibel *et al* [13].

The cross sections for the formation of molecular ions are similar, whether the reactants are neutrals or ions, however, they are about 50% larger in the first case.

One could be tempted to explain the similarity in a simple way. Indeed, the potential energy curves of the ionic state and of the covalent states asymptotically correlated to the

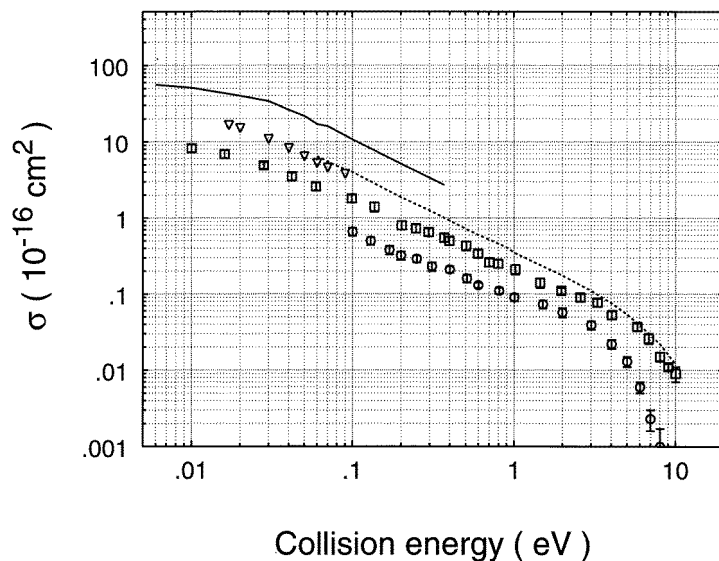


Figure 4. Comparison of the cross sections for associative ionization in the collision of ionic and neutral species. Open circles are our data for $\text{He}^+ + \text{H}^-$. Open squares are our data for $\text{He}^+ + \text{D}^-$. Open triangles are the experimental data of Fort *et al* for $\text{He}^* + \text{H}$. The broken curve is for the experimental data of Neynaber and Magnuson for $\text{He}^* + \text{D}$ and the full curve for the calculation of Waibel *et al* for $\text{He}^* + \text{H}$.

neutral reactants have a crossing near $7a_0$. At low energy, this crossing will be avoided when starting with neutrals while it will be passed diabatically, at least partly, when the reactants are ions, because of the acquired kinetic energy (4 eV). Thus, below $7a_0$, the collision essentially proceeds along the same channel, the ionic channel which is likely to be the most propitious to autoionization. In this view, we even understand that the cross section is larger with neutral reactants.

The truth, however, is that the ionic state is strongly depopulated before reaching the crossing at $7a_0$ due to the crossings with higher lying covalent states.

We have indeed shown in an earlier calculation [6] that, at energies below 10 eV, the electron transfer reaction



strongly populates the 3^3S , 3^3P , 3^1P , 2^3P , and 2^1P states of He but almost never the 2^3S metastable state. It is also clear that the 2^3S cannot dominate the associative ionization. If it did, the cross section for reaction (11) at energy E would have to be of the same order as that of reaction (16) at energy $E + 4$ eV, because of the kinetic energy gained (4 eV) by the ionic reactants before reaching the crossing at $7a_0$; this is obviously not the case.

The rate of associative ionization is determined by the electron–electron interaction and by the nuclear matrix elements coupling the bound states with the vibrational continuum. The electronic interaction is of course smaller for higher states but the nuclear matrix elements become larger because the distance of closest approach is favourably shifted towards the region covered by the nuclear motion in the bound states. This makes the excited covalent channels capable of autoionization.

In conclusion, we believe that the similarity of the cross sections observed for reactions (11) and (16) is purely accidental, the two reactions actually proceeding along

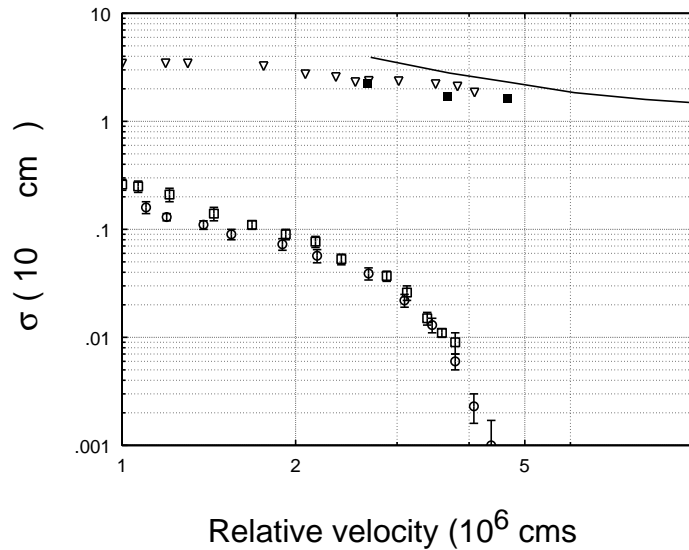


Figure 5. Comparison of the cross section of associative ionization with that of mutual neutralization. The mutual neutralization cross sections have been divided by 100. Full squares and triangles are the measurements of the mutual neutralization by Olamba *et al* [5] and Peart and Hayton [3], respectively. The full curve is for its calculation by Chibisov *et al* [6]. Open squares and circles are the present results for associative ionization of He^+ with D^- and H^- respectively.

quite different channels.

Further it can be noted that the decreasing of the associative ionization cross section, before becoming faster than the E_{cm}^{-1} law above 3 eV, is first slowed down in the range 0.7–3 eV (see figure 2). This could be due to the formation of the $^3\Sigma$ state of the molecular ion which becomes possible above 0.67 eV, as already discussed by Yousif *et al* [17] in the context of the dissociative recombination of HeH^+ .

Finally, the present measurements show that the associative ionization cannot explain the discrepancy appearing between the mutual neutralization cross sections calculated by Chibisov *et al* [6] and measured by Olamba *et al* [5] and Peart and Hayton [3]. This is illustrated in figure 5 where the discrepancy is seen to be larger by at least three orders of magnitude than the cross section for associative ionization. The possibility remains that the discrepancy can be attributed to the contribution of the transfer ionization reaction as suggested before [6]:



However this still has to be checked by measurements of the corresponding cross sections.

References

- [1] Gaily T D and Harrison M F A 1970 *J. Phys. B: At. Mol. Phys.* **3** 1098
- [2] Peart B, Bennett M A and Dolder K 1985 *J. Phys. B: At. Mol. Phys.* **18** L439–44
- [3] Peart B and Hayton D A 1994 *J. Phys. B: At. Mol. Opt. Phys.* **27** 2551–6
- [4] Ermolaev A M 1992 *J. Phys. B: At. Mol. Opt. Phys.* **25** 31–3

- [5] Olamba K, Szücs S, Chenu J P, Naji El Arbi and Brouillard F 1996 *J. Phys. B: At. Mol. Opt. Phys.* **29** 2837–46
- [6] Chibisov M, Brouillard F, Chenu J P, Cherkhani M H, Fussen D, Olamba K and S Szücs 1997 *J. Phys. B: At. Mol. Opt. Phys.* **30** 991–1011
- [7] Howard J S, Riola J P, Rundel R D and Stebbings R F 1973 *J. Phys. B: At. Mol. Phys.* **6** L109
- [8] Magnuson G D and Neynaber R H 1974 *J. Chem. Phys.* **60** 3385–7
- [9] Neynaber R H and Magnuson G D 1975 *J. Chem. Phys.* **62** 4953
- [10] Hickman A P 1977 *J. Chem. Phys.* **67** 5484–90
- [11] Fort J, Laucagne J J, Pesnelle A and Watel G 1977 *10th Int. Conf. on the Physics of Electronic and Atomic Collisions* (Paris: Commissariat A L'Energie Atomique) Abstracts p 302
- [12] Neynaber R H and Tang S Y 1978 *J. Chem. Phys.* **69** 4851–8
- [13] Waibel H, Ruf M W and Hotop H 1988 *Z. Phys. D* **9** 191–207
- [14] Orel A E, Kulander K C and Rescigno T N 1995 *Phys. Rev. Lett.* **74** 4807–10
- [15] Orel A E and Kulander K C 1996 *Phys. Rev. A* **54** 4992–6
- [16] Strömholm C, Semaniak J, Rosen S, Danared H, Datz S, Van der Zande W and Larsson M 1996 *Phys. Rev. A* **54** 3086–94
- [17] Yousif F B, Mitchell J B A, Rogelstad M, Le Paddelec A, Canosa A and Chibisov M I 1994 *Phys. Rev. A* **49** 4610
- [18] Olamba K, Szücs S, Chenu J P and Brouillard F 1997 *20th Int. Conf. on the Physics of Electronic and Atomic Collisions (Vienna)* Scientific program and abstracts of contributed papers FR200